A Cd-based complex as multifunctional fluorescent probe for the detection of Fe^{3+}, ceftriaxone sodium (CRO) and L-aspartic acid (L-Asp)

Jian-Fei Song,[a] Jia-Li Chen,[a] Gui-Quan Guo,[b] Hong-Yan Zhu,[a] Si-Ying Zhou,[a] Xin-Rong Zheng, [a] Xiu-Qing Zhang*[a]

Author information

Corresponding Author

Xiu-Qing Zhang* Email: glutchem@163.com

Orcid ID

Jian-Fei Song: https://orcid.org/0009-0005-3841-9899
Jia-Li Chen: https://orcid.org/0009-0003-3154-318X
Gui-Quan Guo: https://orcid.org/0000-0003-0821-003X
Hong-Yan Zhu: https://orcid.org/0009-0008-1390-6318
Si-Ying Zhou: https://orcid.org/0009-0003-0478-077X
Xin-Rong Zheng: https://orcid.org/0009-0003-8099-7276
Xiu-Qing Zhang: https://orcid.org/0000-0002-2863-8140

a. Guangxi Key Laboratory of Electrochemical and Magneto-chemical Functional Materials, College of Chemistry and Bioengineering, Guilin University of Technology, Guilin 541006, P. R. China.
b. School of Chemical Engineering and Biotechnology，Xingtai University，Xingtai 054001, P. R. China.
†E-mail: glutchem@163.com (X.-Q. Zhang), telephone and fax numbers: +86-0773-2535678;
Electronic Supplementary Information (ESI) available: CCDC 2404074.

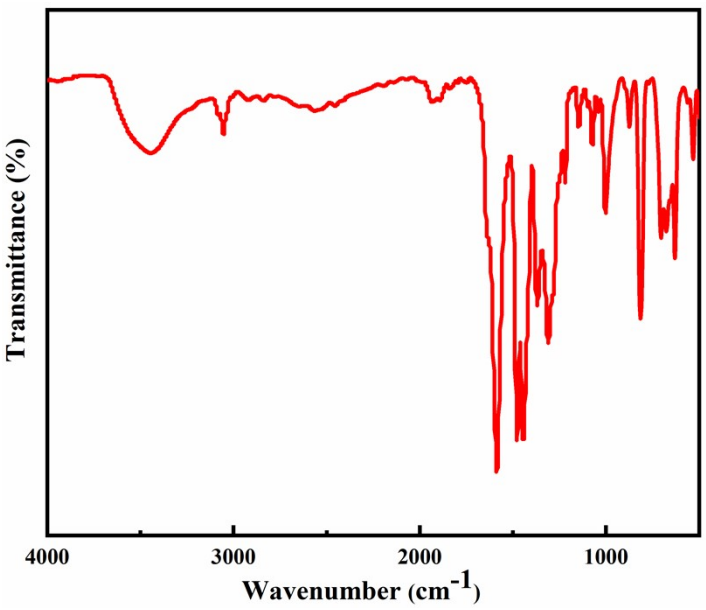

Fig.S1 IR spectra of complex **1**

Table S1. Crystal data and structure refinement for complex **1**

Identification code	**1**
Empirical formula	$C_{49}H_{34}Br_4Cd_2N_6O_{11}$
Formula weight	1427.26
Temperature/K	293(2)
Crystal system	triclinic
Space group	$P\bar{1}$
a/Å	10.88120(10)
b/Å	12.43520(10)
c/Å	20.2017(2)
α/°	96.6730(10)
β/°	94.8020(10)
γ/°	90.3810(10)
Volume/Å^3	2705.07(4)
Z	2
ρ_{calc}g/cm^3	1.752
μ/mm^{-1}	10.278
F(000)	1388.0
Reflections collected	38094
Independent reflections	10970 [R_{int} = 0.0710, R_{sigma} = 0.0613]
Data/restraints/parameters	10970/0/653

Goodness-of-fit on F^2	1.072
Final R indexes [I>=2σ (I)]	R_1 = 0.0592, wR_2 = 0.1706
Final R indexes [all data]	R_1 = 0.0635, wR_2 = 0.1758

Table S2 Selected Bond Lengths (Å) and Angles (°) for **1**

Bond Lengths (Å)			
Cd1—O1	2.308 (3)	Cd2—O7	2.343 (4)
Cd1—O2A	2.339 (3)	Cd2—O8B	2.369 (4)
Cd1—O4	2.344 (4)	Cd2—O10	2.310 (4)
Cd1—N1	2.296 (4)	Cd2—N6	2.281 (4)
Cd1—N4	2.272 (4)		
Bond Angles (°)			
O1—Cd1—O2A	125.71 (13)	N4—Cd1—O5	97.16 (16)
O1—Cd1—O4	147.06 (17)	N4—Cd1—N1	173.37 (15)
O1—Cd1—O5	93.70 (15)	O7—Cd2—O8B	127.95 (13)
O2A—Cd1—O4	87.21 (16)	O10—Cd2—O7	137.96 (13)
O2A—Cd1—O5	140.06 (15)	O10—Cd2—O8B	93.95 (13)
O4—Cd1—O5	53.86 (18)	N3C—Cd2—O7	88.69 (15)
N1—Cd1—O1	87.81 (14)	N3C—Cd2—O8B	91.19 (15)
N1—Cd1—O2A	86.96 (14)	N3C—Cd2—O10	87.01 (15)
N1—Cd1—O4	95.97 (17)	N6—Cd2—O7	92.20 (15)
N1—Cd1—O5	88.55 (17)	N6—Cd2—O8B	87.26 (16)
N4—Cd1—O1	88.44 (14)	N6—Cd2—O10	93.17 (15)
N4—Cd1—O2A	90.79 (14)	N6—Cd2—N3C	178.45 (16)
N4—Cd1—O4	90.14 (17)		

Symmetry codes: (A) -x+2, -y+1, -z+1; (B) -x+1, -y+1, -z+2; (C) x-1, y, z+1; (D) x+1, y, z-1.

Table. S3 Main Hydrogen Bonds for **1**

D-H	Acceptor	d(D-H)	d(H•••A)	d(D•••A)	∠D-H•••A
N2-H2	O11	0.86	2.06	2.910(6)	170
O3-H3	O2	0.82	1.84	2.531(6)	142
N5-H5	O12	0.86	2.12	2.958(7)	163
O6-H6	O5	0.82	1.98	2.635(101)	136
O9-H9A	O7	0.82	1.87	2.577(7)	144
O12-H12	O11	0.82	1.83	2.555(7)	146
C4-H4	O5	0.93	2.57	3.491(8)	171
C15-H15	O7	0.93	2.56	3.208(7)	127
C22-H22	O3	0.93	2.55	3.196(7)	127
C41-H41	Br3	0.93	2.75	3.632(6)	158
C49-H49	O10	0.93	2.49	3.400(7)	166

Table S4. SHAPE analysis of Cd(II) ion in **1**.

	CdO_4N_2	CdO_3N_2
Coordination modes	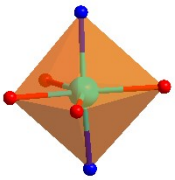	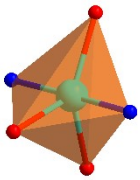
label	OC-6	TBPY-5
symmetry	O_h	D_{3h}
shape	Octahedron	Trigonal bipyramid
Calculation results	Distortion(τ_{min})	
	Cd1 (5.396)	Cd2 (1.702)

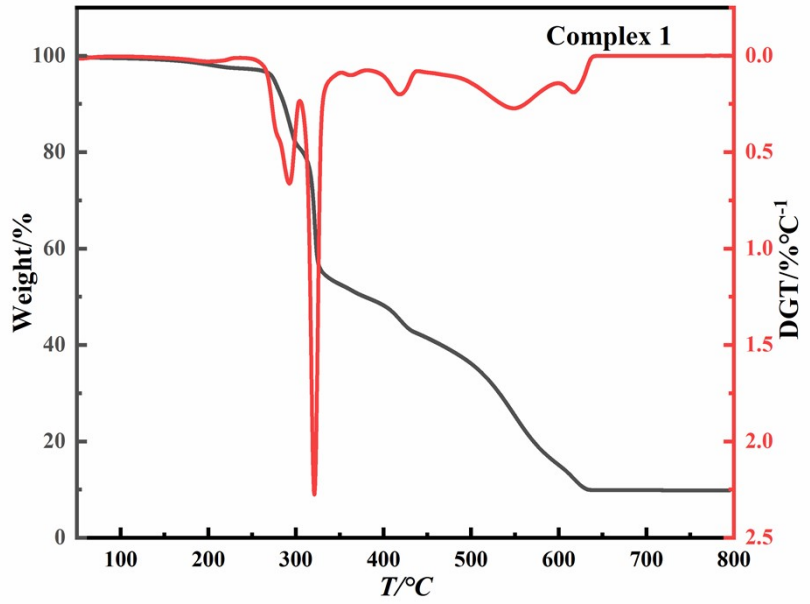

Fig.S2 The TGA curves of complex **1**

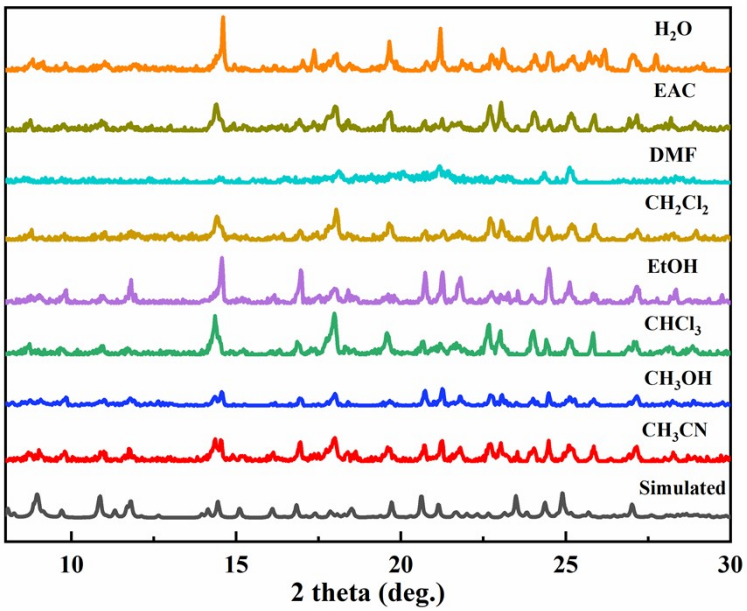

Fig.S3 PXRD spectra of complex **1** in different solvents

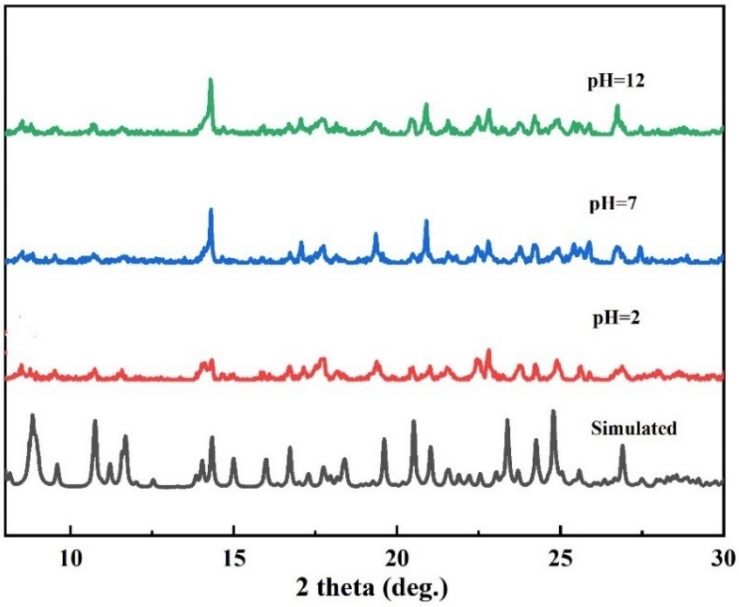

Fig.S4 PXRD spectra of **1** in solutions with different pH values

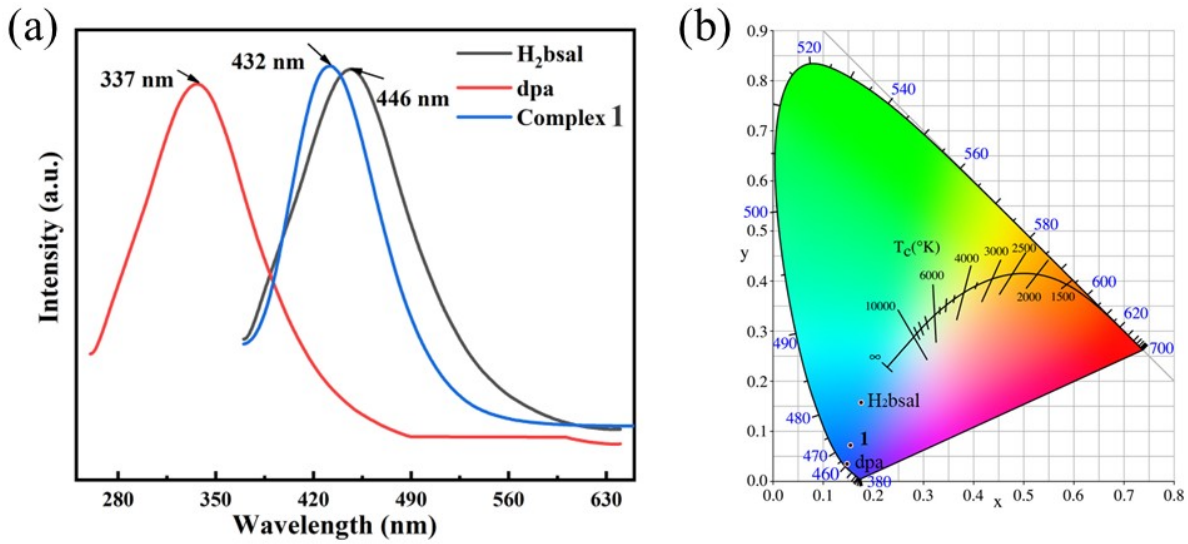

Fig.S5 (a) the fluorescence properties of complex **1**. (b) CIE chromaticity coordinates of **1** and ligand

Ksv and LOD calculation methods

The quantitative fluorescent quenching efficiency of **1** (for analyte) using the Stern−Völmer (S−V) equation.[1]

$$(I_0/I) = 1 + K_{SV}\,C \text{ ---------} (1),$$

Where I is the fluorescence intensity at analyte concentration of C, and I_0 signifies the initial fluorescence intensity of complex **1**. The quenching constant is indicated by K*sv* (M^{-1}). A linear curve is obtained in a relatively definite range of analyte concentration. The equation

$$LOD = 3\sigma/Ksv \text{ ---------} (2),$$

(where σ signifies the standard deviation of the initial fluorescence intensity of complex **1**) was used to calculate the detection limit of analyte.

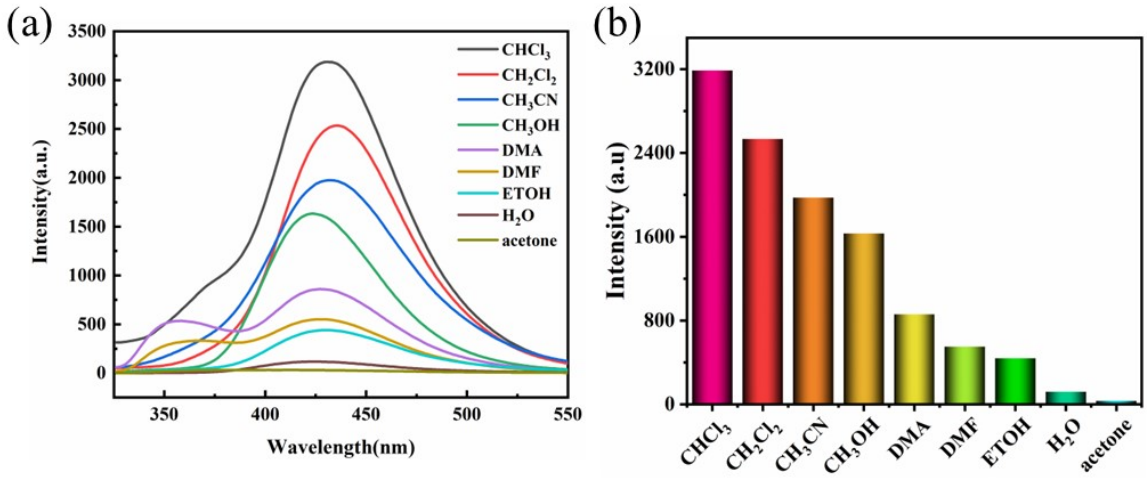

Fig.S6 (a, b) Fluorescence measurements of **1** in various pure solvents.

Tabe S5. Ksv and LOD of MOF-based luminescent sensors for Fe^{3+}, CRO, L-Asp

MOF-based fluorescent materials	Analyte	Quenching constant (M^{-1})	Detection limits	Recycle ability	Ref
$[Cd_2(Hbsal)_4(dpa)_2]_n$	Fe^{3+}	7.5×10^5	1.08 μM	yes	**This work**
$[Cd_2(H_2O)(4\text{-}PDCA)_2]_n$	Fe^{3+}	2.72×10^3	9.8 μM		2
$[Tb_2(L)_3]\cdot2H_2O$	Fe^{3+}	1.74×10^4	0.51 μM	yes	3
$Zn(C_{22}H_{12}N_4O_4)\cdot16H_2O$	Fe^{3+}	1.61×10^4	1.68 μM		4
$[Cd_2(Hbsal)_4(dpa)_2]_n$	CRO	1.43×10^6	0.64 μM	yes	**This work**
$[Cd(IPA)(3dpu)]_n$	CRO	2.49×10^5	0.96 μM	yes	5
$[Cd(bbi)_2(H_2L)_2]_n$	CRO	3.51×10^5	5.5 μM	yes	6
L-Cys-ZnS	CRO	1.57×10^4	5 μM		7
$[Cd_2(Hbsal)_4(dpa)_2]_n$	L-Asp	1.2×10^5	6.25 μM	yes	**This work**
$[Cd_{1.5}(NTB)(bipy)_{0.5}]_n$	L-Asp	2.24×10^6	2.68 μM	yes	8
$[Zn(Aze)(bmbp)]_n$	L-Asp	2.22×10^5	5.33 μM		9
$[Cd(Aze)(bmbp)]_n$	L-Asp	2.88×10^5	2.62 μM		9
Eu/Gd(TCPP)	L-Asp		18 μM		10

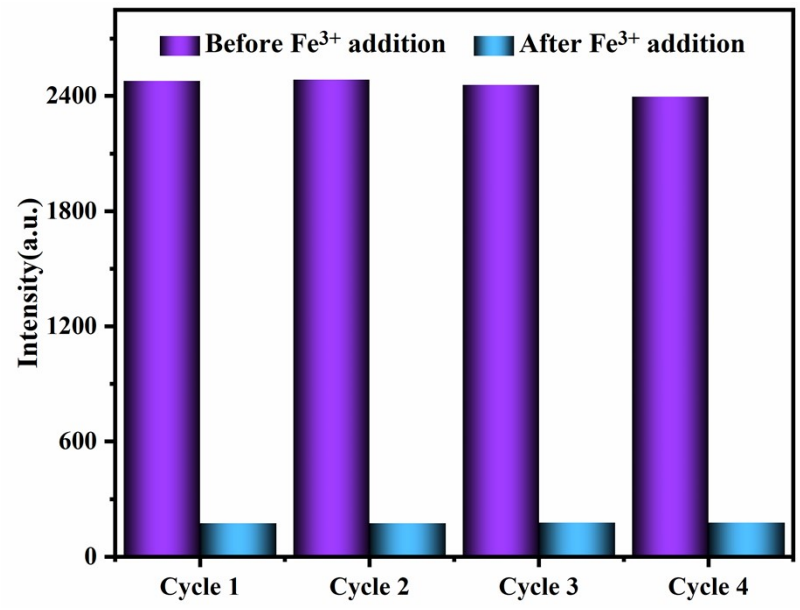

Fig.S7 The cycling experiments of **1**-Fe^{3+}

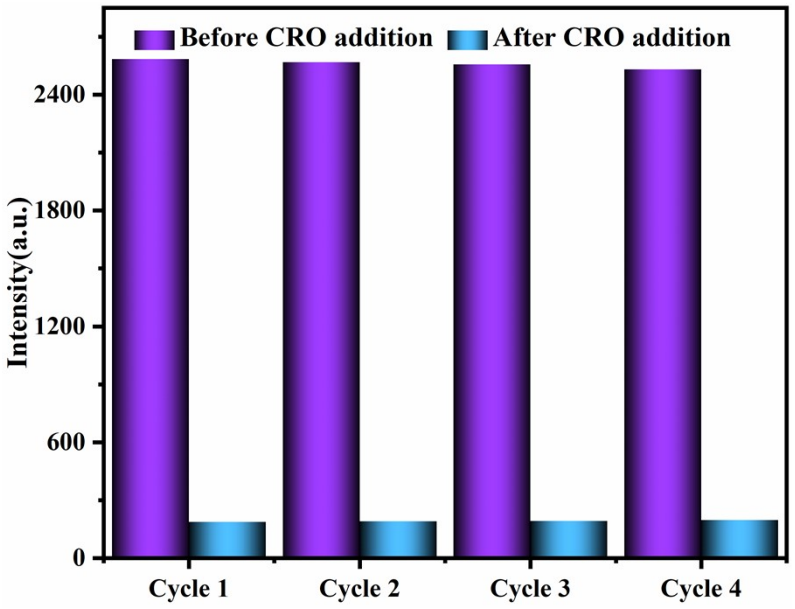

Fig.S8 The cycling experiments of **1**-CRO

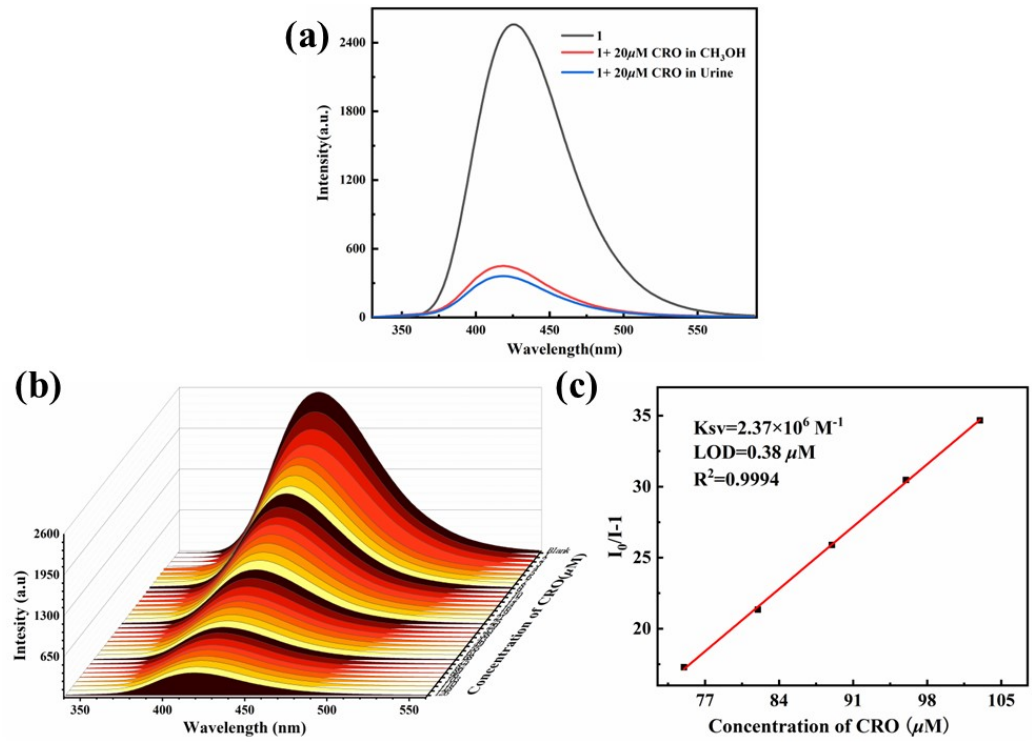

Fig.S9 (a) The fluorescence spectrum of CRO solution added to **1** CH_3OH solution. (CRO was doped in normal human urine for experiment) (b) Emission spectra of **1** dispersed in CH_3OH solutions with increasing concentration of CRO. (CRO in Urine) (c) The Stern-Volmer plot for CRO. (CRO in Urine).

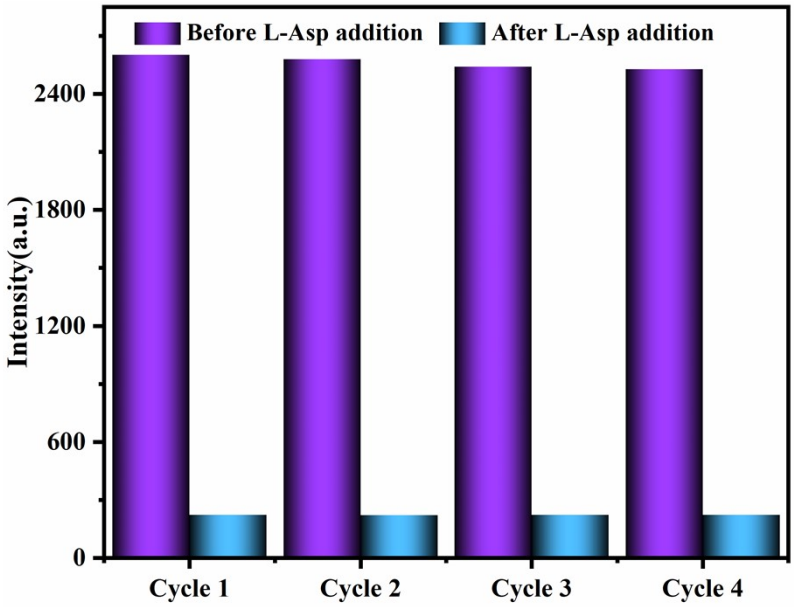

Fig.S10 The cycling experiments of **1**-L-Asp

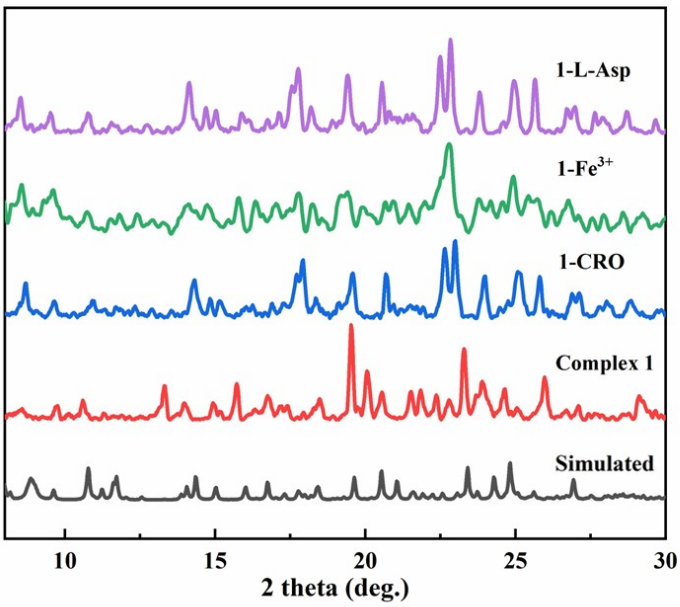

Fig.S11 PXRD spectra of **1**-Fe^{3+}, **1**-CRO and **1**-L-Asp after fluorescence quenching experiments.

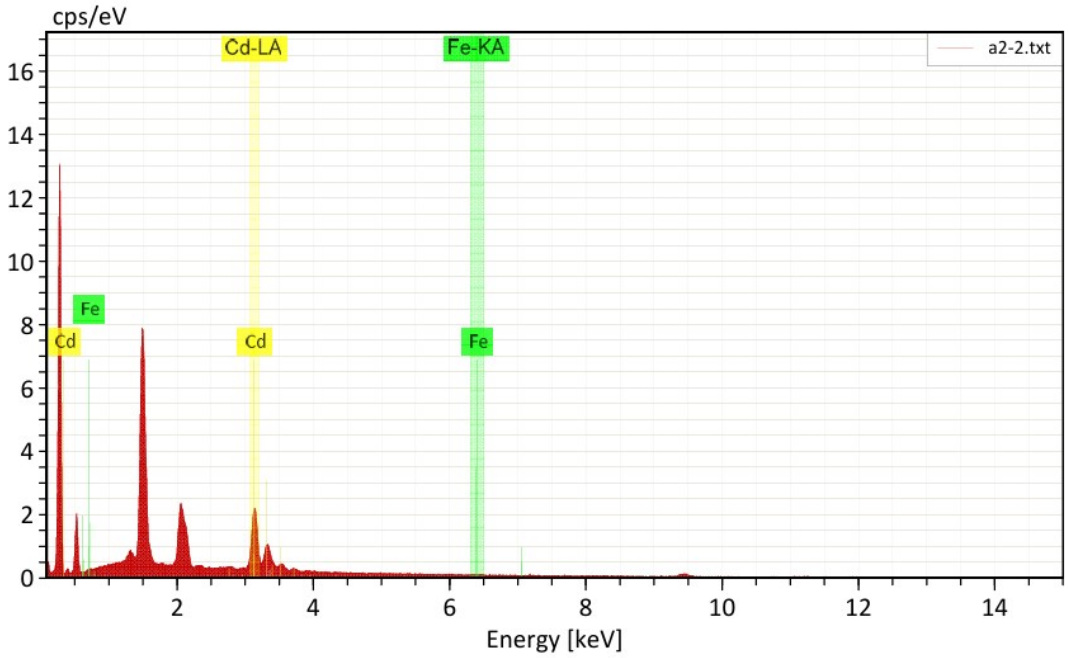

Fig.S12 EDS spectrum of **1**-Fe^{3+}

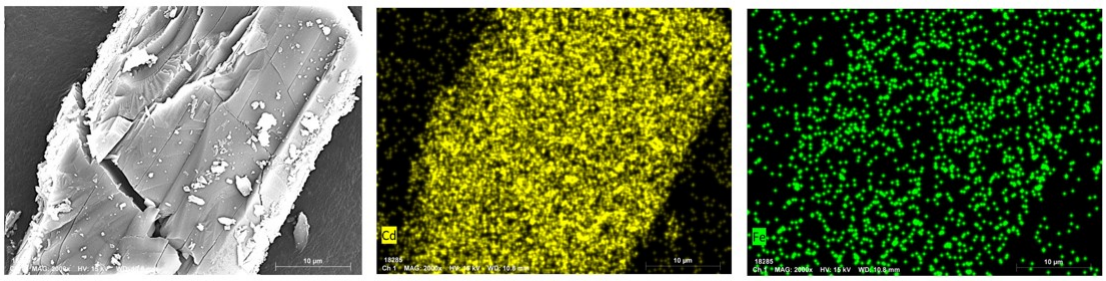

Fig.S13 SEM images and elemental mapping images of **1**-Fe^{3+}

Table S6. The ICP results of complex **1**-Fe^{3+} after luminescent recycles

	Amount of Cd	Amount of Fe
Complex **1**-Fe^{3+} after recycling	13.94 mg/L	0.25 mg/L

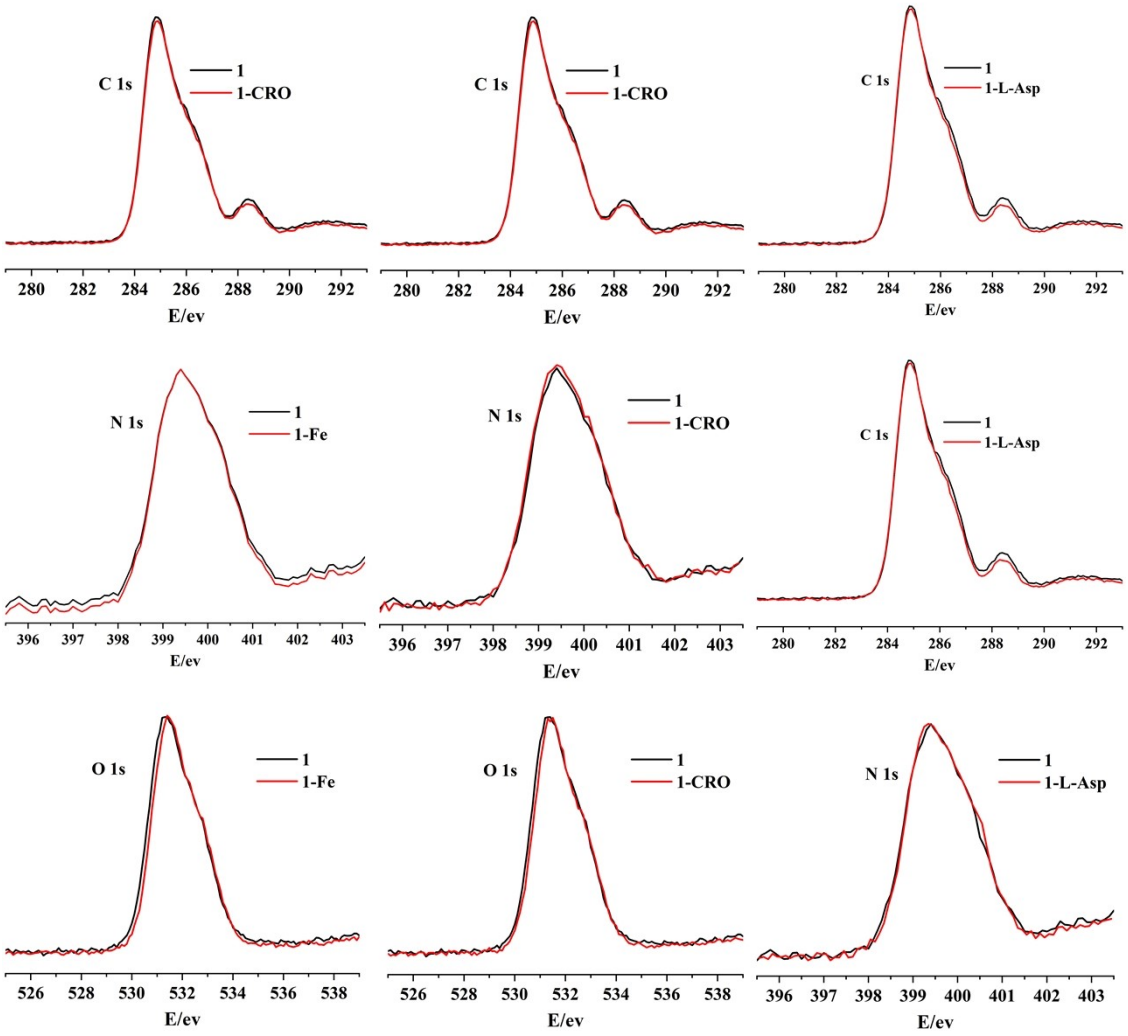

Fig.S14 The XPS spectra of **1** before and after by treating with Fe^{3+}, CRO and L-Asp, respectively (C 1s, N 1s, and O 1s).

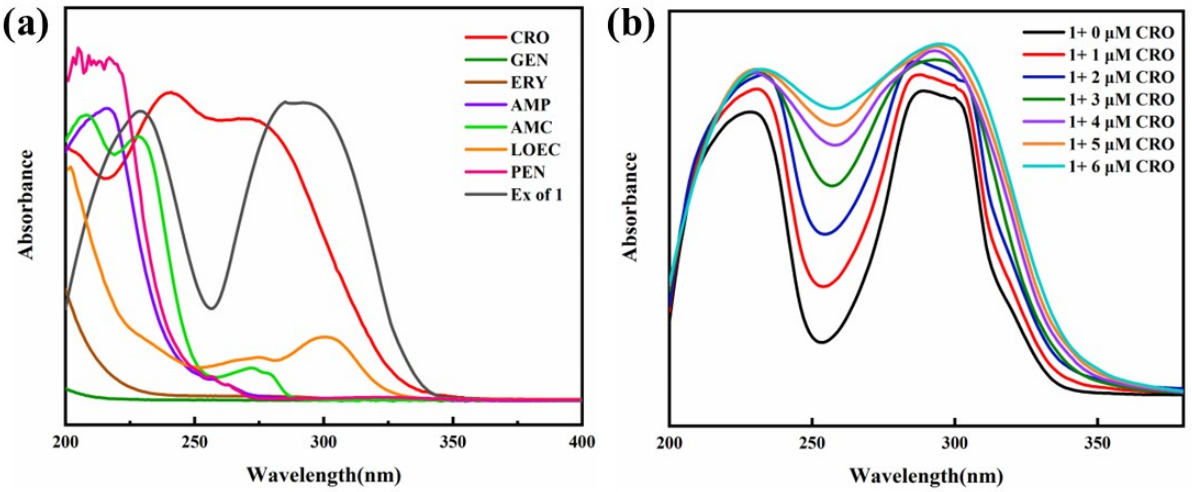

Fig.S15 (a) UV–Vis spectral profiles of different antibiotics recorded in H_2O solution and Ex of **1** in CH_3OH. (b) UV-Vis absorption spectra of **1** upon addition of different concentrations of CRO

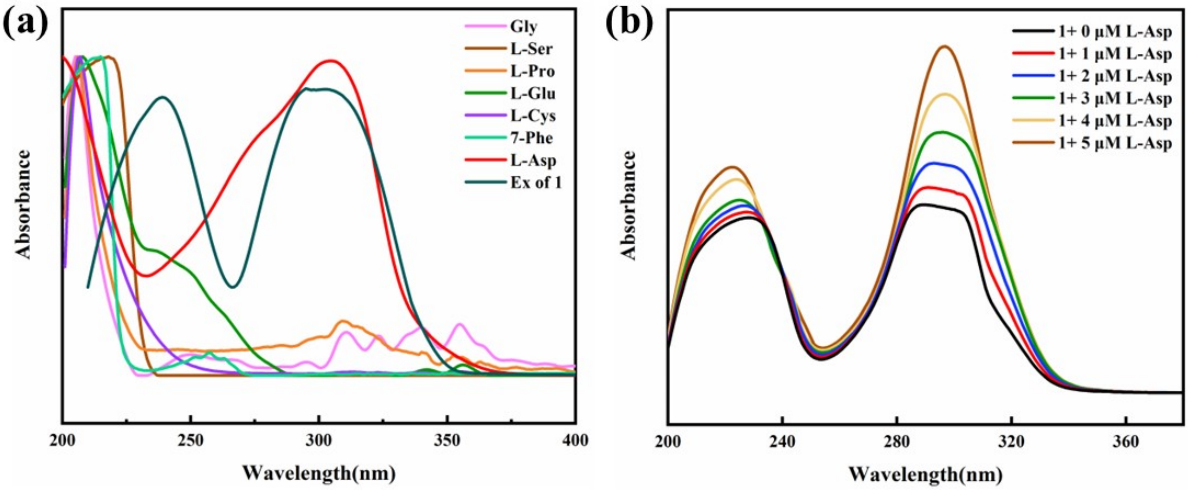

Fig.S16 (a) UV–vis spectral profiles of different amino acids recorded in H_2O solution and Ex of **1** in CH_3OH. (b) UV-vis absorption spectra of **1** upon addition of different concentrations of L-Asp

References

1. H.-F. Liu, T. Ye, X.-H. Qin, C. Chao, F.-P. Huang, X.-Q. Zhang and H.-D. Bian, *CrystEngComm*, 2022, **24**, 1622-1629.
2. J.-H. Gao, P.-P. Huang, Z.-J. Zhang, F.-W. Tian, J. Ge, X.-Y. Cao, J. Liu, D. Wang, N. Zheng, J.-F. Lu, B. Liu, *J. Mol. Struct.*, 2024, **1299**, 137162.
3. C.-Y. Zhu, M.-T. Shen, H.-M. Cao, M.-J. Qi, P. Li, L. Chen, Y. Ge, W. Gao, X.-M. Zhang, *Microchem. J.*, 2023, **188**, 108442.
4. R. Yang, X. Yu, B. Xu, W. Yao, V.-P. Fedin, A.-S. Potapov, E. Gao, *Polyhedron*, 2023, **243**, 116535.
5. Q. Wen, J.-L. Chen, J.-F. Song, S.-Y. Zhou, H.-Y. Zhu, X.-Q. Zhang, *J. Mol. Struct.*, 2024, **1300**, 137235.
6. P. Xing, D. Wu, J. Chen, J. Song, C. Mao, Y. Gao, H. Niu, *Analyst*, 2019, **144**, 2656-2661.
7. K. Wang, X. Gu, N. Deng, L. Li, Y. Ye, Y. Ma, *J. Mol. Struct.*, 2025, **1321**, 139975.
8. H. Yang, D. Qi, X. Si, Z. Yan, L. Guo, C. Shao, W. Zhang, L. Yang, *J. Solid State Chem.*, 2022, **310**, 123008.
9. F.-H. Zhao, Y.-S. Li, Z.-H. Zhao, R. Feng, Z.-L. Li, *Polyhedron*, 2024, **255**, 116963.
10. X. Wen, C. Li, Z. Zhou, Y. He, J. He, X. Hou, *Talanta*, 2023, **265**, 124778.